

L.Ya. Aranovich · R.G. Berman

# Optimized standard state and solution properties of minerals

## II. Comparisons, predictions, and applications

Received: 14 September 1994 / Accepted: 20 March 1996

**Abstract** Internally consistent thermodynamic data for endmembers and solid solutions derived in Part I of this work are used to predict phase relationships and compositions of solid solutions in good agreement with direct experimental observations that were not used in the calibration. This “external” consistency with a large body of experimental observations increases confidence in applications to both petrogenetic grid and thermobarometric calculations. The predicted position of the univariant FMAS equilibrium  $Gt+Cd=Opx+Si+Qz$  occurs between 7.8 kbar – 700° C and 10.6 kbar – 1100° C, in excellent agreement with available phase equilibrium reversals, and with thermobarometric results for both higher-*P* Opx+Si+Qz bearing and lower-*P* Cd bearing granulites. In these assemblages, garnet composition is an excellent geobarometer and  $Al_2O_3$  content of Opx is an excellent geothermometer, almost independent of other compositional variables. Comparison of temperature estimates from different exchange and net-transfer reactions for a number of samples representative of high-grade terranes demonstrates the ability of carefully chosen portions of Fe–Mg minerals to preserve information regarding a high temperature steady state during their evolution. The equilibrium  $Fs+Ok=Alm$ , based on the  $Al_2O_3$  content of Opx, offers the most robust thermometry for the Opx–Gt assemblage because of its relative insensitivity to late Fe–Mg exchange. Applications of this thermometer indicate that in many samples the  $Al_2O_3$  content of Opx yields very similar temperatures to Gt–Cd Fe–Mg exchange. For some high temperature samples, these temperatures are up to 150° C higher than calculated with the Gt–Opx Fe–Mg exchange thermometer.

### Introduction

Since the pioneering works of Karpov et al. (1976) and Helgeson et al. (1978), there has been a great deal of focus on the use of internally consistent thermodynamic data for quantitative petrologic calculations (e.g. Powell and Holland 1985, 1988; Holland and Powell 1990; Berman 1988, 1991). While experimental phase equilibrium studies have provided the foundations for quantitative understanding of igneous and metamorphic rocks, thermodynamic data provide the means to extrapolate from the laboratory to nature. This extrapolation is particularly important and challenging for calculation of phase relationships in complex chemical systems (e.g. Aranovich 1983, 1991) which afford closer approximations of natural systems than the simplified systems most amenable to producing interpretable experimental data. Extrapolation is also important for geothermobarometry calculations in which the deviations of mineral compositions from those produced in experimental studies are significant, and the *P*–*T* range of experimental accessibility is often well removed from the physical conditions of rock equilibration. The potential drawback of the internally consistent approach to quantitative calculations is that the data may not represent all experimental results sufficiently well to meet the most stringent extrapolation requirements. It is therefore important to demonstrate that no loss of accuracy is introduced compared to the use, for example, of a geothermometer based solely on the results of one experimental study. We show in the companion paper (Berman and Aranovich 1996; referred to as Part I) that the combination of derived standard state and mixing properties represents most experimental observations within the uncertainty of the measurements; we suggest that our calibration based on data for many different equilibria results in an increase in overall accuracy over that obtainable from more limited data sets that, in most cases, cannot separate between the standard and mixing energy contributions. This accuracy can also not be obtained from sets of endmember ther-

L.Ya. Aranovich  
Institute of Experimental Mineralogy, Chernogolovka, Russia

R.G. Berman (✉)  
Geological Survey of Canada, 601 Booth Street,  
Ottawa, Ontario, Canada K1A 0E8

Editorial responsibility: K. Hodges

modynamic data that are not linked with mixing properties through appropriate analysis of experimental data (Berman 1988; Holland and Powell 1990).

In this paper we explore some of the geological implications of the optimized thermodynamic data for olivine, orthopyroxene, garnet, cordierite, and ilmenite. We first present calculated phase relationships in complex chemical systems that serve as a basis for consideration of many features in high-grade metamorphic assemblages of pelitic to intermediate composition, and compare these calculations with natural observations. Comparison with available experimental data will also serve as additional tests of the thermodynamic data derived in Part I. We then discuss the implications of the thermodynamic data for thermobarometric calculations for the same assemblages.

### Calculated phase relations

All computations were performed on a PC-486 with the Gibbs free energy minimization software, THERIAK, described by de Capitani and Brown (1987). Thermodynamic data are those described in detail in Part I combined with internally consistent data for other minerals and fluids given by Berman (1988).

#### Phase relations involving ilmenite

Comparisons with experimental data discussed in Part I indicate that our derived properties for the ilmenite solid solution with low hematite component ( $<0.03 X_{\text{Hm}}^{\text{max}}$ ) yield reasonable representation of the energetics on the Ilm-Gk (see abbreviations in Table 1, part I) binary. Predicted phase relationships involving ilmenite provide an opportunity to further test our calibration, in addition to exploring some implications for geothermobarometry. Koziol and Bohlen (1992) examined displacement of the GRAIL equilibrium:



through addition of MgO, and concluded that Fe–Mg mixing in garnet is very near ideal. They report incorporation of up to approximately 2 weight %  $\text{TiO}_2$  in run product garnet, while Bohlen et al. (1983), in studying equilibrium (a) in the Mg-Free system, considered  $\text{TiO}_2$  in garnet analyses to be due to dispersed Rt inclusions. Because of the ambiguity between these observations, we did not use the data of Koziol and Bohlen (1992) in the calibration described in Part I. Predicted phase relations show excellent agreement with the experimental observations (Fig. 1). The garnet side of the divariant loop lies within the uncertainties of, but at slightly less Fe-rich compositions than those determined by Koziol and Bohlen, consistent with the calculations which do not account for solution of  $\text{TiO}_2$  in garnet.

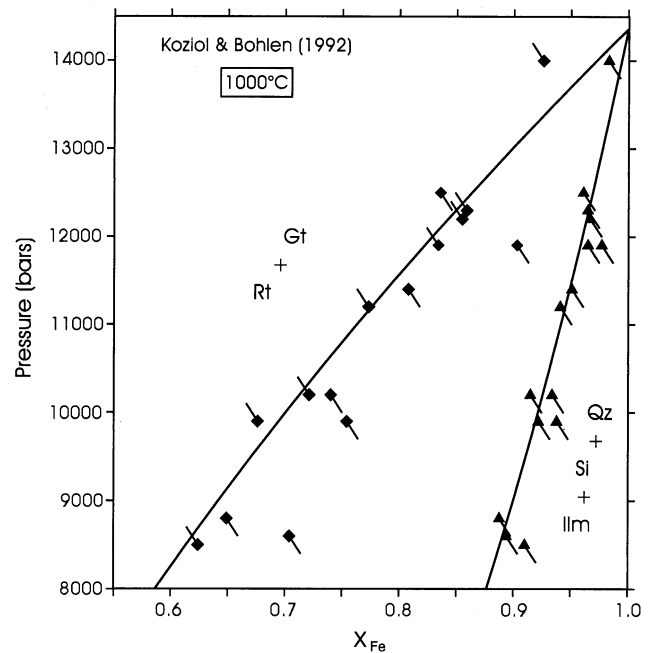


**Fig. 1** Comparison of available experimental data with  $P$ – $X_{\text{Fe}}$  diagram for the divariant assemblage Gt–Ilm–Rt–Si–Qz in the FMAST system, computed with Part I thermodynamic data. Symbols show nominal experimental data, with diamonds and triangles showing Gt and Il compositions, respectively. Lines connected to symbols show effect of  $+0.01 X_{\text{Fe}}$  compositional uncertainties as well as direction from which final compositions were approached

Although Koziol and Bohlen (1992) did not attempt to reverse the Fe–Mg partitioning between garnet and ilmenite, the consistency of their experimental observations (Fig. 1) suggests a close approximation to equilibrium. Koziol and Bohlen (1992) note that their data yield  $K_D=4.9$ , while Green and Sobolev (1975) measured  $K_D$  values around 4.0 in synthesis experiments on pyrolyte and olivine-basanite compositions. Our calculations are in reasonable agreement with both these studies, with  $K_D$  increasing from 3.6 to 5.2 as  $X_{\text{Fe}}$  increases from 0 to 1.

A similar compositional dependence of  $K_D$  is computed for Fe–Mg exchange between Opx and Il. At  $1000^\circ\text{C}$ ,  $K_D$  increases from 8 to 13 going from  $X_{\text{Fe}}=0$  to 1. At higher temperatures, this compositional dependence is reduced as the ilmenite solid solution becomes closer to ideal. Our calculated  $K_D$  values reproduce within uncertainties the  $800$ – $1100^\circ\text{C}$  measurements of Hayob et al. (1993) which were utilized in Part I, as well as the majority of the  $800$ – $1300^\circ\text{C}$  data of Bishop (1980) which were not included in the Part I calibration (Fig. 2). Although only two bulk compositions were studied, the latter data clearly show the large compositional dependence of  $K_D$ , which is important to account for in accurate thermodynamic calculations. One half-bracket of Bishop's at  $1000^\circ\text{C}$  indicates much higher  $K_D$  than our predictions and than the data of Hayob et al. This half-bracket appears to represent a large overstepping of the equilibrium composition produced by the use of highly metastable

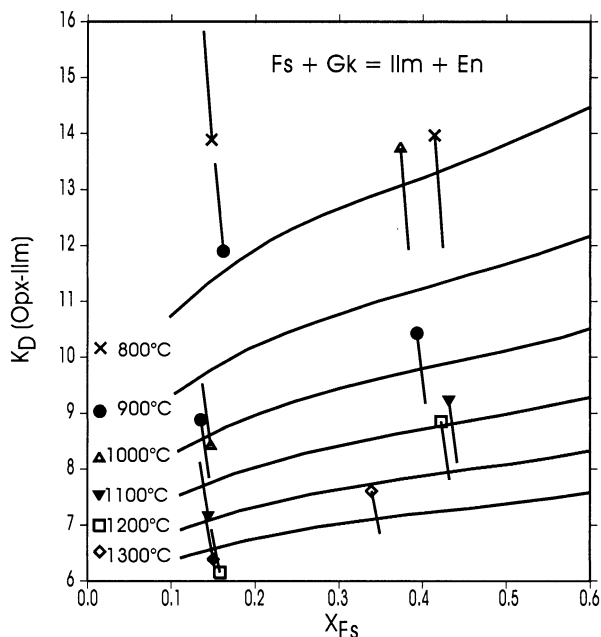


**Fig. 2** Variation of  $K_D$  with  $X_{Fs}$  at 13 kbar for the equilibrium  $Gk+Fs=En+Ilm$ . Symbols as in Fig. 1

starting materials consisting of a mixture of endmember geikilite+ferrosilite.

The above comparisons indicate that ilmenite properties derived in Part I afford very reasonable approximation of phase equilibrium data involving low  $Fe^{3+}$  ilmenite. Fe–Mg exchange thermometers have been proposed for the pairs Ol-II (Andersen et al. 1991) and Opx-II (Bishop 1980). The partitioning of Fe–Mg between Il and Cd is even more extreme, presenting an attractive possibility for geothermometry, albeit limited by the low concentration of Mg in ilmenite at low temperature. Our calculations again show that deviations from ideality in these phases lead to a strong compositional dependence with  $K_D$  increasing from ¥45–75 over the range  $X_{Fe}=0$  to 1 at 600° C and from ¥18 to 30 over the same compositional range at 800° C.

#### Stability of orthopyroxene+olivine (+/-quartz)

Figure 3 shows calculated Fe–Mg exchange isotherms for coexisting olivine-orthopyroxene over the temperature range 400–800° C. In accord with the experimental data on which they are in large part based (von Seckendorff and O'Neill 1993), our calculations indicate (1) a very small temperature dependence of  $K_D$ , which reflects the lack of suitability of this exchange couple as a geothermometer, and (2) that Ol is more Fe-rich than Opx at all temperatures above 700° C. Crossover of the computed isotherms with the diagonal line representing equal partitioning of Fe and Mg between Ol and Opx, such that Ol becomes less Fe-rich than Opx, has been inferred from some natural observations (see references listed in Sack and Ghiorso 1989) and from older experi-

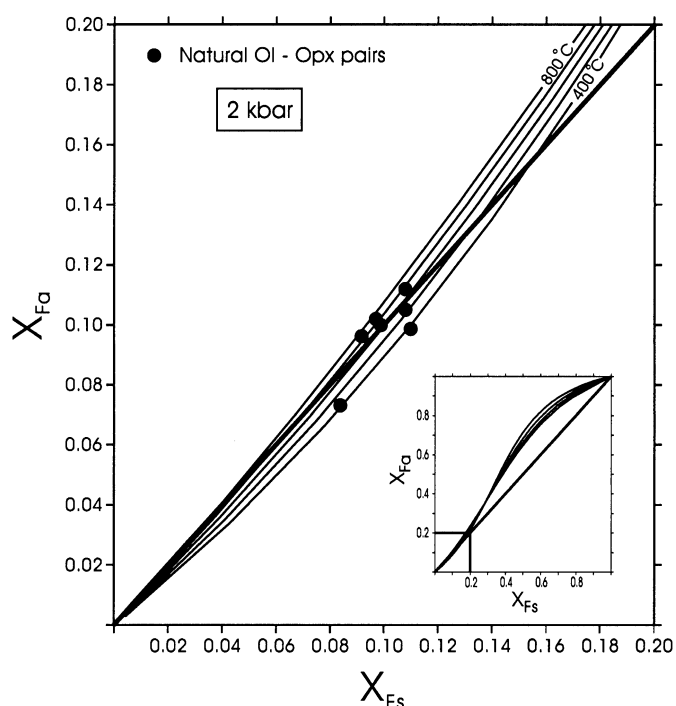


**Fig. 3** Mg-rich portion of computed Roseboom diagram for Ol–Opx at  $P=2$  kbar, and 400–800° C. Inset shows isotherms over entire compositional range. Compositions of natural coexisting Ol+Opx (filled circles) taken from compilation by Sack and Ghiorso (1989). Note that for  $X_{Fe}<0.10$ , Part 1 systematics predict  $X_{Fe}^{Opx}>X_{Fe}^{Ol}$  at temperatures below 800° C

mental studies (Medaris 1969; Matsui and Nishizawa 1974; Fonarev 1987; Koch-Mueller et al. 1992). Reasons for the apparent disagreement with these experiments have been discussed in detail by von Seckendorff and O'Neill (1993). We can add to their arguments that only two experimental points with  $X_{Fe}^{Ol}<X_{Fe}^{Opx}$  ( $X_{Fe}^{Ol}=0.11$ , 900° C;  $X_{Fe}^{Ol}=0.11$ , 1000° C, Koch-Mueller et al. 1992) are inconsistent with the calculated isotherms (Fig. 3) in terms of direction of approach to equilibrium (see discussion in Part I). These inconsistencies can be attributed to experimental difficulties such as X-ray determination of final compositions, and possible lack of equilibrium due to extreme sluggishness of the reactions with starting Mg-rich Opx. Apparent disagreement with the natural observations deserves more detailed consideration.

According to our calculations there is a point, at approximately  $X_{Fe}^{Opx}=0.28$  (see inset in Fig. 3), of intersection of the exchange isotherms, which divides them into two parts with the opposite temperature dependence (i.e. with the opposite sign of the integral enthalpy change of the exchange reaction). Such a crossover point was not observed in the experiments of von Seckendorff and O'Neill (1993), but it is not precluded by them either (cf. runs 41, 42, 13/1, 13/2, 1/1, 33, 38, and 34 in their Table 2). Low-temperature extrapolation of our fit for these extremely Mg-rich compositions produces a crossover with the diagonal (Fig. 3) at temperatures below ca.

700° C. For natural samples with  $X_{Fe}^{Ol}$  less than or equal to  $X_{Fe}^{Opx}$  (compositions taken from Sack and Ghiorso 1989, their Table A1), our calculations predict equilibration temperatures in the range 400–750° C, in broad agreement with the geological environments in which they formed (serpentinites and tectonically emplaced peridotites). These samples may well have undergone a process of low temperature reequilibration, rather than representing complete disequilibrium due to different reaction rates of Ol and Opx with a hypothetical Mg-reservoir as suggested by von Seckendorff and O'Neill (1993).

The olivine-orthopyroxene-quartz assemblage was one of the first quantitatively calibrated geobarometers (Bohlen et al. 1980; Bohlen and Boettcher 1981), and our calculations (Fig. 4) confirm its validity as a geobarometer. It should be noted that, although our predicted olivine composition in equilibrium with orthopyroxene+quartz at any specific temperature is slightly less Fe-rich than determined in these studies (see Part I), the position of the Fe/(Fe+Mg) isopleths on a  $P$ - $T$  diagram (Fig. 4) coincides well with those determined experimentally by Bohlen and Boettcher (1981).

In spite of the fact that the Opx isopleths have a very shallow  $dP/dT$  slope, suggesting a minimal temperature dependence of pressure readings for this geobarometer, there is an indirect influence of temperature. For example, a rock with bulk Fe/(Fe+Mg)=0.8 equilibrated at 800° C and 4 kbar should contain  $X_{Fe}^{Opx}$ =0.78 and  $X_{Fe}^{Ol}$ =0.88 (Fig. 4, see also Fig. 7, Part I). Low-tempera-

ture Fe–Mg resetting down to 600° C (without operation of the net-transfer reactions) would change coexisting compositions to  $X_{Fe}^{Opx}$ =0.76 and  $X_{Fe}^{Ol}$ =0.90, leading to a pressure determination of less than 2 kbar (Fig. 4). This implies that pressure estimates from the Ol–Opx–Qz assemblage in rocks subjected to slow cooling may correspond to a minimum rather than peak metamorphic pressure.

#### Stability of orthopyroxene+magnetite+quartz

The equilibrium:



limits the maximum Fe-content of Opx at oxygen fugacities above that of the QFM buffer, and is important as a “oxybarometer” for high-grade metamorphic rocks of a variety of bulk compositions (Fonarev 1987). Experimental observations on the composition of Opx equilibrated with Mt and Qz at temperatures between 700 and 850° C, pressures of 1 and 5 kbar, and  $f_{\text{O}_2}$  buffered by Ni–NiO were reported by Fonarev et al. (1976) and Fonarev (1987). These data are important for independent assessment of the mixing properties of Opx on the En-Fs join, as well as the standard state properties of ferrosilite. They were not incorporated into the analysis of Part I because of ambiguities in the experimental determination of Opx composition. Contradictory interpretations have been given to the data by Fonarev (1987) and Lindsley (1980); the former suggesting a positive  $dT/dX_{Fe}$  slope of the phase boundary, and the latter a negative slope.

Figure 5 shows  $T$ - $X_{Fe}$  sections at two pressures that were experimentally investigated, calculated for this assemblage with the thermodynamic parameters derived in Part I. Our systematics predict a very slight negative  $T$ - $X_{Fe}$ , a rather diplomatic compromise to Lindsley's (1980) and Fonarev's (Fonarev et al. 1976; Fonarev 1987) interpretations. More importantly, however, our calculations are consistent with the experimental obser-

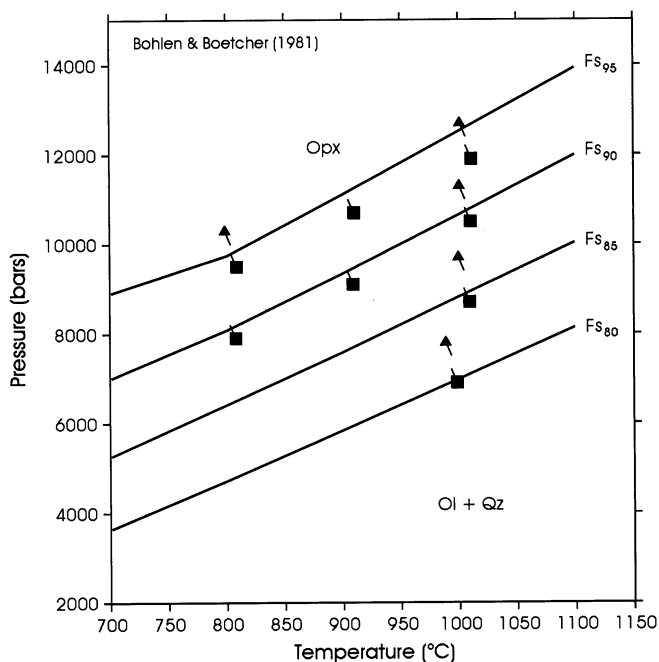


**Fig. 4** Comparison of computed isopleths of Opx (labelled at 5 mol% Fs intervals) with experimental observations by Bohlen and Boettcher (1981). Triangles show  $P$ - $T$  conditions, adjusted for experimental uncertainties, at which Opx of the corresponding Fs content was found stable. Squares show conditions where Opx broke down to the divariant assemblage Opx+Ol+Qz. Opposite ends of attached lines show nominal experimental  $P$ - $T$  conditions

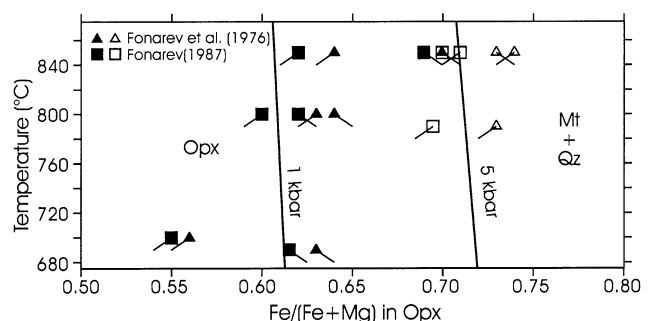


**Fig. 5**  $T$ - $X_{Fe}$  diagram for the assemblage Opx+Mt+Qz at oxygen fugacities buffered by Ni–NiO and pressures of 1 and 5 kbar. Labelled curves calculated with thermodynamic data from Part I. Symbols as in Fig. 1, with data at 1 kbar (solid symbols) and 5 kbar (open symbols) of Fonarev et al. (1976, triangles) and Fonarev (1987, squares)

vations on compositional changes of Opx during the course of reaction (b), particularly if the compositions of Opx reported by Fonarev (1987), rather than those reported in the earlier publication (Fonarev et al. 1976), are taken.

### Garnet-orthopyroxene phase relations in CMAS

Experimental observations on stability of pyrope-grossular garnet relative to Opx+An+Sil in the quartz-saturated portion of the system CMAS (Hensen 1976; Perkins 1983) were not included in the thermodynamic data retrieval described in Part 1, and provide an independent test for the derived garnet solution properties as well as standard properties of the minerals involved. The position of the univariant curve together with computed  $X_{Gr}^{Gt}$  and  $X_{Al_2O_3}^{Opx}$ , are shown in Fig. 6. Agreement between our calculations and independent experimental results is reasonably good. Our calculations indicate 7% grossular component at 1300°C and 15.3 kbar (Fig. 6), in excellent agreement with experimental observations (6–7% grossular) at the same  $P$ – $T$  conditions (Perkins 1983). Our calculated curve is at slightly lower pressure than the lowest temperature brackets obtained by Perkins (1983), but is consistent with Hensen's (1976) data. On the basis of their own thermodynamic analysis, the valid-

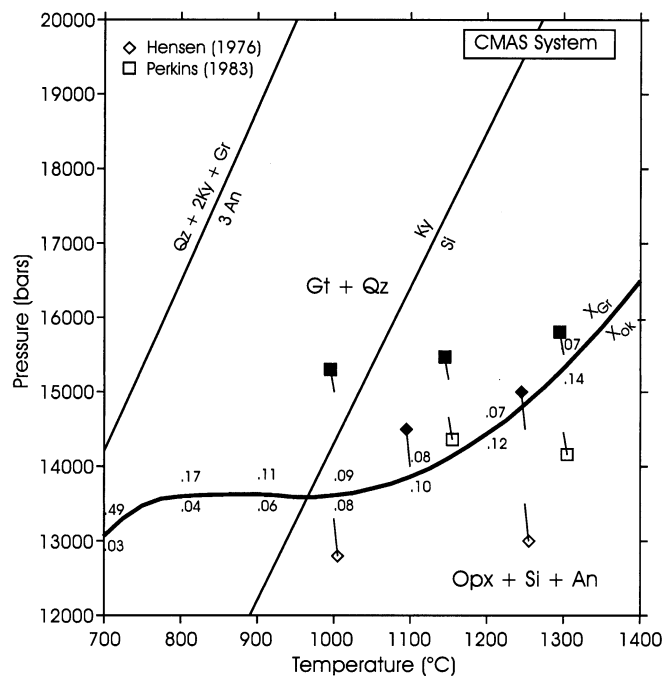


**Fig. 6** Comparison of experimental observations by Hensen (1976, diamonds) and Perkins (1983, squares) in the system CaO–MgO–Al<sub>2</sub>O<sub>3</sub>–SiO<sub>2</sub> with univariant curve (bold) for the equilibrium  $Gt+Qz=Opx+An+Sil/Ky$ , calculated with thermodynamic data of Part I. Numbers above and below the curve show  $X_{Gr}$  and  $X_{Ok}$ , respectively. Symbols as in Fig. 4. Pronounced curvature of the reaction is caused by compositional degeneracy in which the Ca:Mg ratio in Gt becomes identical to that of the assemblage Opx+An at  $X_{Gr}=0.33$

ity of Perkins' brackets was questioned by Perkins (1983) and Wood and Holloway (1984).

Some peculiarities of the univariant boundary are worth noticing here: the strong variation in the curvature of the univariant boundary, and the significantly lower solubility of grossular component on the sillimanite side of the curve. Both these features stem from the fact that the univariant reaction is the "extremal" type (Prigogine and Defay 1954; Korzhinskii 1973). At a certain bulk composition, reactions of this type become degenerate, involving a lesser number of phases than in the general case. For the reaction under consideration this composition is close to  $Py_{67}Gr_{33}$ , where Al<sub>2</sub>SiO<sub>5</sub> is not needed to balance the reaction. Small deviation from this composition is caused by appreciable solubility of Al<sub>2</sub>O<sub>3</sub> in Opx.

### Garnet-orthopyroxene-cordierite phase relationships in FMAS

The  $P$ – $T$  diagram portraying phase relations between garnet, orthopyroxene and cordierite +/- sillimanite, quartz (Fig. 7) has many important implications as well as representing an extremely sensitive test of thermodynamic properties derived in Part I. The principal feature of this diagram is the univariant curve separating Opx+Si from Gt+Cd assemblages in silica-saturated rocks. The lowest pressure of this boundary, computed with the data of Part I, is approximately 8 kbar, indicating the relatively high pressure origin of hypersthene-sillimanite-quartz gneisses described in many ancient granulite-facies terranes (Harley 1989 and references

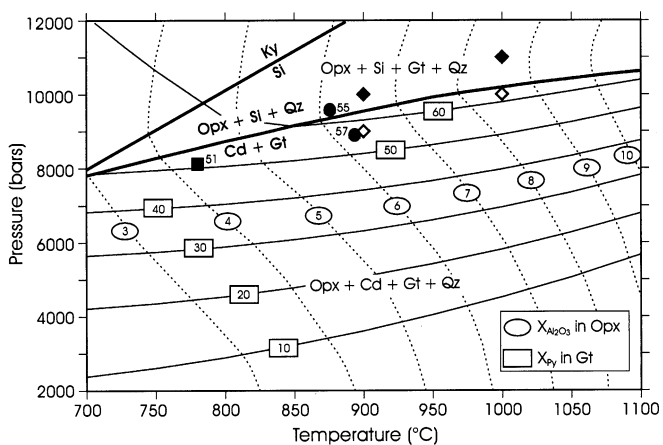


**Fig. 7**  $P$ – $T$  grid for the assemblage  $Gt+Cd+Opx+Sil+Qz$  in the system MgO–FeO–Al<sub>2</sub>O<sub>3</sub>–SiO<sub>2</sub>. Curves computed with Part I thermodynamic data (with fully hydrated cordierite) show univariant equilibrium (bold curve), as well as isopleths of 100  $X_{Fe}^{Gt}$  (numbers inside boxes) and Al<sub>2</sub>O<sub>3</sub> content of Opx (1 mol% intervals, ovals).  $P$ – $T$  positions of natural samples with the most Mg-rich Gt (Mg# = 51) in the assemblage  $Gt+Opx+Crd+Qz$  and the most Fe-rich Gt (Mg# = 57) in the assemblage  $Gt+Opx+Sil+Qz$  are plotted as filled square and circles, respectively. Solid and open diamonds show nominal experimental brackets (assuming 10% friction correction for talc pressure cells) for the univariant equilibrium from Bertrand et al. (1991)

therein). It also shows that formation of the Opx–Si–Qz assemblage is restricted to metapelite compositions with relatively high bulk Mg/(Mg+Fe) ratios (>0.5). Although generally similar to the previously published grids (Aranovich and Podlesskii 1989; Hensen and Harley 1990), our calculations (Fig. 7) differ from the previous studies in some important details. First, we predict the transition at 1–2 kbar lower pressure, and correspondingly more Fe-rich garnet composition along the univariant curve. According to our calculations the lower limit for Mg# of garnet equilibrated with Opx+Si+Qz is about 50, compared to 70 calculated by Aranovich and Podlesskii (1989) and about 65 inferred by Hensen and Harley (1990). Support for the grid presented here comes from reports of garnet as low in Mg# as 57 and 55 (circles in Fig. 7) in Opx–Si–Qz gneisses from the Aldan Shield (Perchuk et al. 1985; Aranovich and Podlesskii 1989) and Varpaisjarvi, Central Finland (Holtta et al., work in preparation), respectively. In addition, the predicted univariant boundary is in excellent agreement with high-temperature reversals on this reaction obtained by Bertrand et al. (1991). Unfortunately, run products of this study were compositionally extremely heterogeneous, preventing meaningful comparisons with our predicted compositions.

Our calculated compositions of Opx and Cd along the univariant curve do not reveal the maxima in Mg# suggested by Hensen and Harley (1990). Rather they show a steady increase in Mg# with increasing temperature. The computed curvature of the univariant boundary is also not as pronounced as that proposed by Hensen and Harley (1990). The “extremal” nature of the curve (a pressure maximum exists above 1100° C) is dictated in this case by the fact that the bulk Mg/(Mg+Fe) ratio of the low pressure assemblage Gt+Cd becomes equal to that of Opx.

Garnet Mg# in the divariant assemblages Gt+Cd+Opx+Qz, Gt+Cd+Sil+Qz and Gt+Opx+Sil+Qz is extremely sensitive to pressure variations (Fig. 7) and, therefore, can be used as a geobarometer independent of any other compositional parameters. The only cause for caution is in the pressure dependence of the isopleths on the activity of cordierite which itself depends on water activity. Our calculations show that the garnet isopleths, which correspond to the divariant equilibrium Gt+Qz=Opx+Cd, can be a maximum of 2 kbars lower in pressure in the limiting case of anhydrous cordierite.

Cordierite stability is known to be significantly influenced by the presence and composition of a fluid phase (e.g. Newton 1972; Aranovich and Podlesskii 1989). Both dry ( $P_{\text{fluid}}=0$ ) and pure CO<sub>2</sub> ( $P=P_{\text{CO}_2}$ ) conditions lead to an increased stability field of the Opx+Si+Qz assemblage at the expense of Cd+Gt. It is important to note, however, that at higher pressure, where the solubility of H<sub>2</sub>O and CO<sub>2</sub> molecules in the cordierite structural channels becomes almost identical, the difference between the location of the univariant curve becomes very small, as is well illustrated in the experimental observations by Bertrand et al. (1991).

Isopleths of Al<sub>2</sub>O<sub>3</sub> in orthopyroxene have a negative slope on  $P$ – $T$  diagram (Fig. 7), which differs strongly from the previously published results (Aranovich and Podlesskii 1989; Hensen and Harley 1990). This difference is caused primarily by a significantly lower Al-content in Opx in FAS predicted by the present study in accord with new experimental observations by Aranovich and Berman (1995, 1996). It may have important implications for deciphering reaction textures in high-grade rocks: for assemblages lacking primary Opx, development of Cd+Opx coronas around Gt should be indicative of decompression, while for those having matrix Opx it could be just as well related to cooling. Problems associated with applications of Al-in-Opx thermometry will be further discussed below under “geothermobarometry”.

Cordierite has been reported in textural equilibrium with the assemblage garnet-orthopyroxene-quartz with garnet as magnesian as Mg#=51 (square in Fig. 7; Sutam block of the Aldan Shield; Aranovich 1991) and Mg#=54 (Enderby Land, Antarctica; Ellis et al. 1980). If “fluid-absent” conditions had dominated during granulite-facies metamorphism, the transformation from cordierite- to sillimanite-bearing garnet-orthopyroxene assemblages should have taken place at much more Fe-rich garnet compositions (Aranovich and Podlesskii 1989, their Fig. 5). This implies that at least in some areas a fluid phase was physically present during the high-grade metamorphic event, a conclusion reached also by Hensen and Harley (1990) on similar grounds.

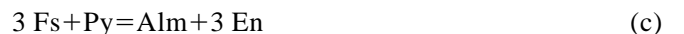
---

## Geothermobarometry implications

In this section we highlight a few implications associated with application of the systematics derived in Part I to deciphering the  $P$ – $T$  conditions of equilibration of high-grade metamorphic assemblages. These calculations have been made using the TWQ software of Berman (1991).

### Garnet-orthopyroxene geothermometer

Geothermometry based on the exchange of Fe–Mg between garnet and orthopyroxene, via the equilibrium:



has been experimentally investigated in several laboratories (Kawasaki and Matsui 1983; Harley 1984; Lee and Ganguly 1988; Eckert and Bohlen 1992). Our calculations summarized in Part I demonstrate that derived thermodynamic properties agree within uncertainties with almost all data from these four studies that involved crystalline starting materials. Because of the use in Part I of the entire combined experimental data set, our calibration for equilibrium (c) is significantly different from any based solely on one set of experiments.

Temperatures computed for coexisting garnet-orthopyroxene pairs in a variety of geologic environments

**Table 1** Temperatures computed for natural samples with the Fe–Mg Opx–Gt exchange equilibrium (c)

Area/Reference	#	Average	Range	$X_{\text{Fe}}^{\text{Gt}}$	$X_{\text{Gr}}^{\text{Gt}}$	$X_{\text{Ox}}^{\text{Opx}}$
Aldan Shield Aranovich (1991)	3	860	825–880	0.35–0.52	0.01–0.02	0.05–0.11
Furua Complex Coolen (1980)	13 12	797 809	652–919 743–919	0.59–0.75 0.59–0.75	0.16–0.17 0.16–0.17	0.02–0.03 0.02–0.03
Asuanipi Complex Percival (1991)	11 10	752 763	643–829 694–829	0.58–0.70 0.58–0.69	0.03–0.04 0.03–0.04	0.05–0.07 0.05–0.07
Oaxaca Mora and Valley (1985)	4	765	700–809	0.72–0.77	0.07–0.19	0.01–0.03
Adirondacks Jaffe et al. (1978)	2	665	619–711	0.98–0.99	0.21	0.003–0.005
Arendal, Norway Lamb et al. (1985)	6	750	720–793	0.66–0.85	0.09–0.19	0.01–0.03
Bamble, Norway Harlov (1992)	10	699	646–746	0.60–0.90	0.02–0.20	0.01–0.06
Adirondacks Jen and Kretz (1981)	5 4	714 680	653–851 653–707	0.85–0.89 0.85–0.87	0.17–0.22 0.18–0.22	0.013 0.013
Antarctica Sandiford /1985)	7 6	708 671	630–988 630–760	0.48–0.82 0.48–0.82	0.02–0.20 0.02–0.20	0.01–0.11 0.01–0.11
Otter Lake Perkins et al. (1982)	3	742	666–844	0.77–0.80	0.18–0.21	0.008–0.009
Minto Block Begin and Pattison (1994)	6 5	691 713	580–800 654–800	0.64–0.79 0.64–0.79	0.03–0.08 0.03–0.08	0.02–0.06 0.03–0.06
Nain Complex Berg (1977)	17 12	811 735	631–1140 631–785	0.64–0.85 0.64–0.85	0.01–0.05 0.01–0.05	0.03–0.06 0.03–0.06

are presented in Table 1. If compositional zoning in garnet and/or orthopyroxene was reported in the original publications, temperature estimates have been calculated using compositions of the cores of the minerals. The results in Table 1 indicate that our systematics produce  $T$  estimates broadly consistent with the petrologic intuition – mineral facies approach. The temperatures obtained for each complex generally fall within  $+75^\circ\text{C}$  of the average value, indicating reasonable clustering of the  $T$ -estimates but not without the effects of late stage reequilibration in some samples. We consider this an encouraging feature of the systematics given the wide range of Gt and Opx compositions covered by the data in Table 1. Especially notable are the temperature estimates for Adirondaks samples with extremely Fe-rich garnet and orthopyroxene ( $X_{\text{Fe}}=0.98\text{--}0.99$ , Jaffe et al. 1978), which are in excellent agreement with temperatures computed for more typical compositions found in the Adirondaks (Johnson and Essene 1982). In general, our computed temperatures average about  $30\text{--}50^\circ\text{C}$  lower than those based on the calibration of Lee and Ganguly (1988).

A central point of contention in recent applications of geothermobarometry concerns the ability of Fe–Mg exchange thermometers to recover “near-peak” temperatures for relatively slow cooled rocks (e.g. Pattison and Newton 1989; Frost and Chacko 1989; Harley 1989; Fitzsimons and Harley 1994; Pattison and Begin 1994). Detailed compositional maps which show large, steep gradients in  $\text{Fe}/(\text{Fe}+\text{Mg})$  at contacts between ferromagnesian minerals, and little to no gradients where garnet is

surrounded or in contact with quartz or feldspar (e.g. Pattison and Begin 1994; Florence and Spear 1991) leave little doubt that low temperature reequilibration via diffusive exchange is a common, if not unavoidable feature in slowly cooled metamorphic rocks. These observations are also supported by theoretical simulations of diffusion profiles in minerals (e.g. Chakraborty and Ganguly 1992). Considerable uncertainty remains, however, regarding the extent to which these low-temperature processes affect core compositions of low-diffusive minerals, in particular garnet, which is involved in the most effective geothermometers. As pointed out by Pattison and Begin (1994), kinetic modelling does not provide an unambiguous solution to this problem because cooling rates of the rocks are unknown and uncertainties of experimentally determined diffusion coefficients are large enough to permit contradictory results from diffusion profile simulations.

Our calculations do not reveal any significant temperature underestimates suggested by some authors to be a typical feature of the Fe–Mg exchange thermometers in high-grade rocks (e.g. Pattison and Newton 1989; Frost and Chacko 1989; Harley 1989), although a certain amount of lower temperature resetting is indicated for a few samples in Table 1 taken by themselves. For less ambiguous conclusions to be drawn, computed Fe–Mg exchange temperatures must be compared with estimates based on a compositional parameter assumed to be more conservative with respect to low-temperature reequilibration. The  $\text{Al}_2\text{O}_3$  content of Opx has been suggested by

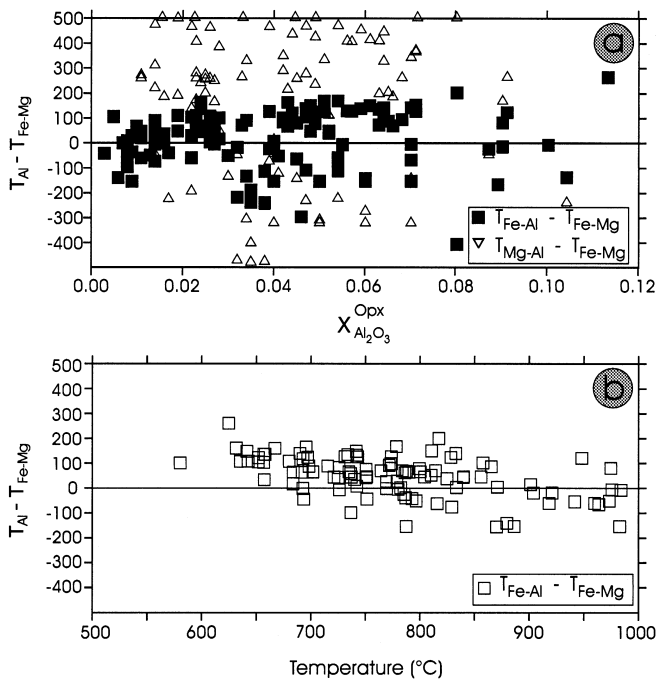
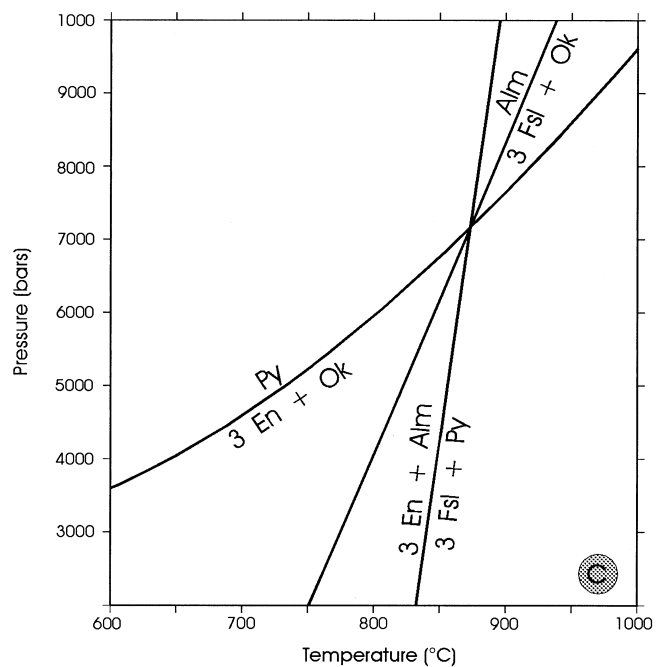


**Fig. 8** Difference between temperatures computed with  $\text{Al}_2\text{O}_3$  content of Opx (squares  $T_{\text{Fe-Al}}$ , triangles  $T_{\text{Mg-Al}}$ ) versus  $X_{\text{Ok}}$  in Opx (a), and  $T_{\text{Fe-Mg}}$  (b). Zero line denotes ideal correspondence of the thermometers. Note the much closer correspondence to  $T_{\text{Fe-Mg}}$  of  $T_{\text{Fe-Al}}$  than  $T_{\text{Mg-Al}}$ . **c**  $P$ - $T$  diagram showing linear dependence among the exchange equilibrium  $\text{Py} + \text{Fs} = \text{En} + \text{Alm}$  and the two net transfer equilibria  $\text{Fs} + \text{Ok} = \text{Alm}$  and  $\text{En} + \text{Ok} = \text{Py}$



many authors (Aranovich and Podlesskii 1989; Anovitz 1991; Fitzsimons and Harley 1994; Pattison and Begin 1994) to be less sensitive to low temperature reequilibration because it is governed by net transfer reactions that have much higher activation energies than the Fe-Mg interdiffusion process.

In order to evaluate these suggestions, we have computed temperatures for the samples in Table 1 not only on the basis of the Fe-Mg exchange equilibrium (c), but also the net transfer equilibria:



Equilibrium (e) has been used extensively as a geobarometer in ultramafic systems (e.g. Finnerty and Boyd 1984) and a geothermometer in more acid compositions (e.g. Pattison and Begin 1994; Fitzsimons and Harley 1994). To our knowledge equilibrium (d) has not been applied previously as a geothermometer. Here we refer to temperatures calculated with equilibria (c), (d) and (e) as  $T_{\text{Fe-Mg}}$ ,  $T_{\text{Fe-Al}}$ , and  $T_{\text{Mg-Al}}$ , respectively.

For the samples in Table 1 we calculated temperatures using all three equilibria. The results of these calculations, expressed as a difference between temperature estimates from the net-transfer and exchange reactions are plotted as a function of  $X_{\text{Al}_2\text{O}_3}$  in Opx (Fig. 8a) and

$T_{\text{Fe-Mg}}$  (Fig. 8b). Observation of Fig. 8a shows that  $(T_{\text{Fe-Al}} - T_{\text{Fe-Mg}})$  is always less than  $(T_{\text{Mg-Al}} - T_{\text{Fe-Mg}})$ , reflecting the fact that these three equilibria are not independent, with reaction (d) having a  $P$ - $T$  slope intermediate between those of (c) and (e) (Fig. 8c). In addition, the larger standard enthalpy change of equilibrium (d) ( $-35.5$  kJ/mol) makes it more robust relative to equilibrium (e) ( $-4.7$  kJ/mol). For these reasons, subsequent discussion will only consider the more reliable temperatures based on  $T_{\text{Fe-Al}}$  and  $T_{\text{Fe-Mg}}$ .

In Figs. 8a and 8b, individual points are rather equally distributed around the zero base line that denotes perfect agreement between the two thermometers, suggesting no tendency of the exchange thermometer to underestimate temperature. About 70% of the squares plot within  $\pm 75^\circ \text{C}$  of the zero base line, demonstrating reasonably good agreement between the two thermometers. That reaction (d) appears to monitor somewhat higher  $T$  values than the exchange reaction (c) (Fig. 8b) reaffirms that the Fe-Mg exchange freezes in at a lower temperature than Al net transfer. On the other hand, one may question whether equilibrium has been attained between Gt and Opx in this temperature range, particularly for the most Fe-rich samples with very low  $\text{Al}_2\text{O}_3$  contents of Opx (see Table 1).  $T_{\text{Fe-Mg}}$  values for these samples range from 770 to 640 $^\circ \text{C}$ , in reasonable agreement with corresponding regional estimates (Johnson and Essene 1982) for the Adirondacks, while  $T_{\text{Fe-Al}}$  is far too low for many samples to be explained with any equilibrium model. For the samples with relatively high  $T_{\text{Fe-Mg}}$ , the net-transfer reaction (d) in many cases gives lower temperatures estimates than the exchange reaction (Fig. 8b).

The ability of Fe-Mg exchange thermometers to recover near-peak metamorphic temperatures in high-grade rocks can be further assessed by detailed compari-

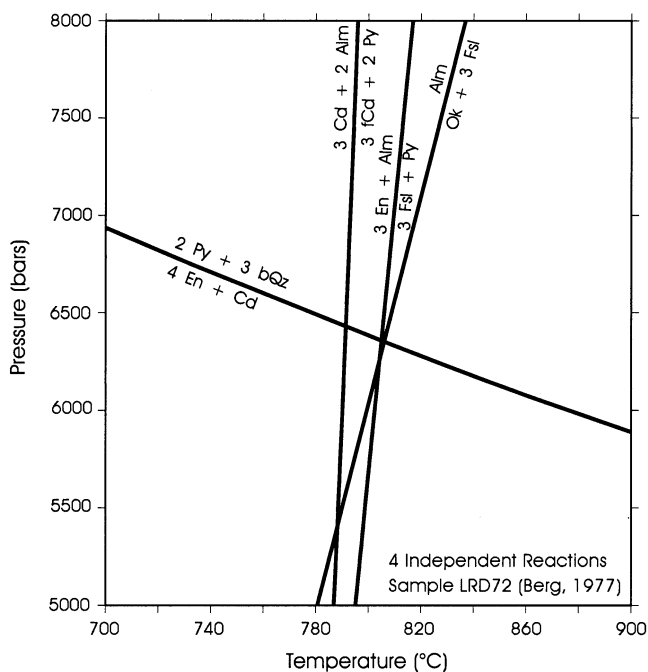


**Fig. 9** Thermobarometric results for sample LRD-72 (Berg 1977) computed with TWQ software and thermodynamic data derived in Part I

sons of the temperature readings of these two thermometers in individual rocks. We performed such tests on well documented samples of Gt+Cd+Opx+Qz gneisses from the contact aureole of the Nain anorthosite massif (Berg 1977), as well as granulites of the Minto block, Northern Quebec (Begin and Pattison 1994) and Aldan shield, Eastern Siberia (Perchuk et al. 1985; Aranovich 1991). Most samples (e.g. Fig. 9) show good agreement between garnet-cordierite and garnet-orthopyroxene exchange temperatures ( $T_2$  and  $T_3$ , respectively, of Table 2), with a general tendency (excluding Nain samples with zoned Gt) towards slightly lower temperatures (0–100° C) for the Gt-Opx thermometer. Gt-Cd exchange temperatures are, however, in excellent agreement with temperatures based on equilibrium (d). As the latter are much less sensitive than the Gt-Opx exchange equilibrium to late Fe–Mg reequilibration, the lower Gt-Opx exchange temperatures may indicate somewhat higher Fe–Mg diffusivity in Opx relative to Cd and Gt in this temperature range.

Several samples of Berg's (1977) give unrealistically high temperatures with both thermometers when core compositions of the garnets were used in the calculations (Table 2). Berg reports that symplectic coronas of Opx+Cd around compositionally zoned garnet are a

**Table 2** Computed  $P$ – $T$  values for selected natural samples<sup>a</sup>

Sample	Ref	$X_{Ok}$	$X_{Py}$	$P_1-T_1$	$T_2 @ P_1$	$T_3 @ P_1$	$P_2-T_4$
LRD-72	Berg (1977)	0.039	0.348	6.4–806	793	805	6.4–797
KI 3557		0.042	0.140	3.0–870	770	875	3.5–820
2-893		0.27	0.188	4.2–780	782	820	4.1–800
2-1833		0.056	0.191	3.4–887	778	785	4.3–780
2-1455 <sup>b</sup>		0.054	0.335	7.2–980	1170	900	7.1–1015
2-1637 <sup>b</sup>		0.054	0.206	4.4–935	920	830	4.8–875
KI 3909		0.048	0.163	3.8–890	855	860	4.1–857
2-625		0.039	0.165	2.8–800	690	750	3.6–725
2-1726		0.034	0.172	3.1–790	710	745	3.6–730
RAW-437		0.026	0.168	2.7–735	645	730	3.1–690
2-1572 <sup>b</sup>		0.047	0.292	6.3–915	990	910	6.2–945
2-1578 <sup>b</sup>		0.032	0.244	5.8–850	985	860	5.5–915
2-1480 <sup>b</sup>		0.039	0.285	6.3–885	1010	890	6.0–945
NK 420B		0.044	0.224	3.9–810	690	755	4.5–725
NU-69		0.043	0.213	3.2–780	635	690	4.2–660
2-275		0.042	0.231	4.1–810	730	735	4.7–735
74-98a		0.047	0.146	2.7–850	725	780	3.5–755
2-1572r		0.044	0.230	4.5–845	780	810	4.8–800
C 10B <sup>c</sup>	Begin and	0.033	0.187	5.6–840	765		
B 69E <sup>c</sup>	Pattison (1994)	0.027	0.188	4.6–745	690		
P 88 <sup>c</sup>		0.040	0.225	7.3–910	812		
P 69 <sup>c</sup>		0.022	0.206	3.2–650	570		
B 74B		0.58	0.346	5.3–800	670	782	6.2–750
B 58		0.046	0.320	4.8–770	650	780	5.9–740
S 2 <sup>d</sup>		0.770	0.344			7.3–775	6.5–772
P 79 <sup>d</sup>		0.731	0.299			6.9–767	6.5–765
KU14316 <sup>e</sup>	Holtta et al. (in prep)	0.090	0.546	7.8–900	795	–	10.2–800
Sut-2	Aranovich	0.049	0.465	7.7–845	850	780	7.8–820
Sut-61 <sup>e</sup>	(1991)	0.091	0.643	9.7–960	890	–	11.2–885
Tok-18 <sup>e</sup>		0.113	0.551	7.8–970	800	–	10.9–830
Tok-18/1 <sup>e</sup>		0.079	0.551	8.4–850	840	–	8.4–842

<sup>a</sup>  $T_1$  computed from  $Fs+Ok=Alm$ ;  $T_2$  computed with Gt–Opx exchange equilibrium;  $T_3$  computed with Gt–Cd exchange equilibrium;  $P_1$  computed with  $Py+Qz=En+Cd$ ;  $T_4-P_2$  computed from intersection of  $P_1$  with  $Alm+Qz=Fs+fCd$  equilibrium.

<sup>b</sup> Samples with strongly zoned garnet;  $P_1$  computed from  $Py+Gr+Qz=En+An$ .

<sup>c</sup> Samples containing Grt+Opx+Pl+Qz;  $P_1$  computed from  $Gr+Py+Qz=En+An$ .

<sup>d</sup> Samples containing Grt+Cd+Sil+Pl+Qz;  $P_1$  and  $P_2$  computed from  $Py+Si+Qz=Cd$  and  $Gr+Si+Qz=An$ , respectively;  $T_4=T_3$ .

<sup>e</sup> Samples containing Grt+Opx+Pl+Qz;  $P_1$  computed from  $Py+Qz=En+Si$ ;  $P_2$  computed from intersection of  $T_2$  and  $P_1$ .

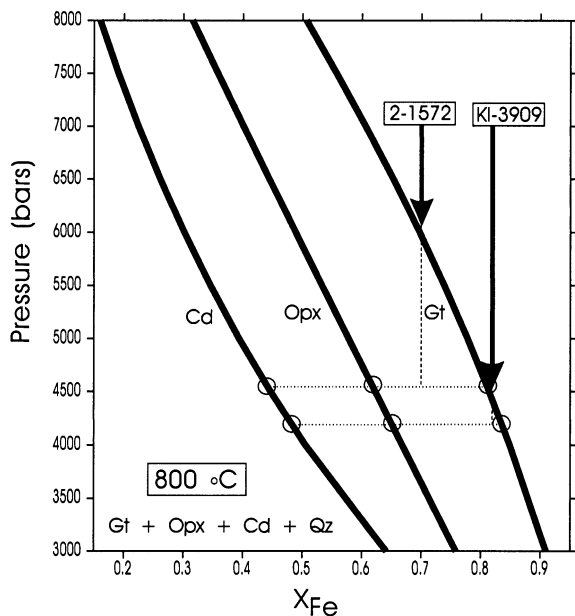


**Fig. 10**  $P$ - $X_{\text{Fe}}$  diagram showing divariant loop for the assemblage Gt-Cd-Opx-Qz. See text for discussion of evolution of two coronitic samples described by Berg (1977)

common feature in these rocks, suggesting their formation in the course of the continuous reaction:



Hence the core compositions of garnets in these samples may be considered as relics of the “starting material”, while those of the outer parts of garnet grains should more closely correspond to equilibrium with Opx and Cd. Details are not given, however, as to which specific samples contain these textural features. For one of the samples (#2-1572), Berg gave a detailed compositional profile of the garnet (Opx and Cd are almost homogeneous). Temperatures calculated on the basis of near-rim compositions (800° C) of minerals for this sample (#2-1572r in Table 2) are much lower than those based on the core compositions (950° C) and agree very well with the estimates from other samples by Berg (1977).

It can be argued that the rim compositions of garnet may not represent the original equilibrium ones because of later-stage cooling undergone by the rocks. Detailed observations show that the late-stage intergranular diffusion caused by such cooling generally affects only the very outer parts of Fe-Mg minerals at their mutual contacts and is readily recognizable by the steep compositional gradient it normally produces (e.g., Berg 1977; Perchuk et al. 1985) as well as close correspondence of compositional changes in the adjacent mineral grains to the progress of the exchange reactions. Compositions of the inner parts of the grains (but still removed from the cores) which exhibit much shallower compositional gradients, or contacts with leucocratic minerals seem to be better candidates for geothermobarometry of corona-bearing samples. In any event employing the core com-

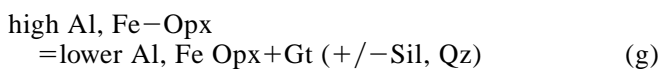
positions of the minerals surrounded by coronas for retrieving  $P$ - $T$  conditions of their formation is unjustifiable and should lead to erroneous conclusions regarding the  $P$ - $T$  evolution of rocks. Conversely, in high-grade rocks lacking prograde zoning and textural evidence of reaction relationships among minerals, it seems reasonable to use core compositions for recovering “near-peak” physical conditions of high-grade metamorphism. Some caution is needed, however, as detailed compositional maps (Pattison and Begin, 1994) indicate that some Fe-Mg reequilibration of Opx and Gt cores may occur in high temperature granulites.

Formation of Opx+Cd coronas is a typical feature of many high-grade metamorphic rocks of the appropriate bulk composition and is usually explained by rapid decompression (e.g. Harley 1989 and references therein). Our systematics suggest that cooling could also be a factor if primary Opx was involved in the corona-forming reaction. A significantly lower Al content of corona Opx relative to that of the matrix Opx would be characteristic in the latter case (see Fig. 7). The samples described by Berg (1977) do not, however, contain primary Opx and therefore their reaction textures should be attributed to decompression. Rocks with different bulk Fe/(Fe+Mg) ratio must initiate reaction during decompression at different pressures. Fig. 9 illustrates this point for several of Berg’s (1977) samples. Sample 2-1572 which has a Gt core composition of Mg# = 30 should start to react to more Fe-rich Gt+Opx+Cd at about 6 kbar, while garnet with Mg# = 18 (sample KI3909) would remain unreacted up to 4 kbar. If core compositions of the garnets were used in  $P$ - $T$  calculations this would have produced an apparent  $P$ -difference between the two samples of about 2 kbar and the erroneous conclusion of a non-isobaric origin of the corresponding parts of the Nain complex. At the same time if the composition of the outer parts (but not the extreme rims affected by low-temperature Fe-Mg exchange) of the garnet in the first sample are taken, both  $T$  and  $P$  estimates for these samples become very similar (800–850° C, 4–4.8 kbar; Table 2). It is noteworthy that the more Fe-rich garnet (KI3909) is almost unzoned (except for the very narrow outer parts of the grains in direct contact with cordierite (Fig. 3 of Berg 1977)). So far as diffusivities of Mg and Fe in garnet are similar (Chakraborty and Ganguly 1992), at least in the limited compositional range of the Fe-rich garnets, the difference in zoning profiles between the two garnets appears to be due to the difference between “starting” (nonequilibrium core) and “final” (equilibrium near-rim) compositions for each of them rather than the difference in the rate of diffusional homogenization. The above example shows also how dangerous could be an attempt to calibrate garnet-orthopyroxene geothermobarometers basing on the naturally occurring assemblages, especially those containing reaction textures.

Two samples (S2 and P79 in Table 2) described by Begin and Pattison (1994) contain the assemblage Gt+Cd+Sil+Pl+Qz. TWQ calculations show very good agreement between Gt-Cd exchange temperatures for

these samples and those that also contain Opx (B74B and B58 in Table 2), as well as with  $T_{\text{Fe-Al}}$  for the latter samples. Gt-Opx exchange temperatures are considerably lower for most samples (up to 130° C), again suggesting susceptibility of Opx to compositional reequilibration at lower temperature. It should be noted, however, that the differences between our results and the two thermometers are not as extreme as Begin and Pattison (1994) calculated on the basis of Harley's (1984) experimental data.

For the Aldan Shield samples containing Gt+Opx +Sil (last three samples in Table 2), our systematics again give  $T_{\text{Fe-Al}}$  higher than those calculated from  $T_{\text{Fe-Mg}}$ , suggesting some resetting of the latter thermometer for these very high temperature rocks. One of the samples (Tok-18, Aranovich and Podlesskii 1989) represents an Archean granulite basement reworked and uplifted during a major Proterozoic event in the Stanovoy fold belt, Eastern Siberia (Karsakov 1978; Perchuk et al. 1985). It is characterized by complex textural features compatible with its long  $P$ - $T$  history (Aranovich and Podlesskii 1989), and also by a very high  $\text{Al}_2\text{O}_3$  content of the core of Opx (11 wt%  $\text{Al}_2\text{O}_3$ ). This composition yields  $T_{\text{Fe-Al}} = \approx 1000^\circ\text{C}$ , which is about 170° C higher than that based on  $T_{\text{Fe-Mg}}$  (Table 2). An alternative explanation to low-temperature Fe-Mg reequilibration could be that garnet was formed in this rock later than Opx by the reaction (Aranovich and Podlesskii 1989):



and, therefore, the core Opx represents a relic composition which never was in equilibrium with garnet and should not be used in Gt-Opx thermobarometry.  $T_{\text{Fe-Al}}$  estimates consistent with  $T_{\text{Fe-Mg}}$ , obtained for this sample from the composition of slightly less coarse-grained Opx (Tok-18/1; Table 2), offer support for this possibility.

## Conclusions

The calculations and discussion presented in this paper demonstrate that the thermodynamic systematics derived in Part I predict phase relationships and compositions of solid solutions in good agreement with direct experimental observations that were not used in the calibration. This "external" consistency with a large body of experimental observations increases confidence in applications to both petrogenetic grid and thermobarometric calculations.

The predicted position of the univariant FMAS equilibrium  $\text{Gt} + \text{Cd} = \text{Opx} + \text{Si} + \text{Qz}$  occurs between 7.8 kbar - 700° C and 10.6 kbar - 1100° C, in excellent agreement with thermobarometric results for both Opx-Si-Qz assemblages with the lowest Mg# and Cd-bearing granulites with the highest Mg#. In these assemblages, garnet composition is an excellent geobarom-

eter and  $\text{Al}_2\text{O}_3$  content of Opx is an excellent geothermometer, independent of other compositional variables.

Comparison of temperature estimates from different exchange and net-transfer reactions for a number of samples representative of high-grade terranes demonstrates the ability of carefully chosen portions of Fe-Mg minerals to preserve information regarding a high temperature steady state during their evolution. Relative insensitivity of the equilibrium  $\text{Fs} + \text{Ok} = \text{Alm}$  to late Fe-Mg reequilibration, makes this new thermometer the most robust for the Gt-Opx assemblage. Applications of this thermometer yield consistent temperature estimates relative to Gt-Cd Fe-Mg exchange temperatures, but somewhat higher temperatures than recorded by the Gt-Opx Fe-Mg exchange thermometer.

**Acknowledgements** We gratefully acknowledge the generous support received by LYA from the Continental Geoscience Division of the Geological Survey of Canada. We also appreciate the helpful review provided by E. Froese. This paper is a contribution to IGCP #304 (Lower Crustal Processes), and is Geological Survey of Canada contribution number 41294.

## References

- Andersen DJ, Lindsley DH (1979) The olivine-ilmenite thermometer. *Proc Loth Lunar Planet Sci Conf. Geochim Cosmochim Acta 1 (Suppl 11):493-507*
- Andersen DJ, Bishop FC, Lindsley DH (1991) Internally consistent solution models for Fe-Mg-Mn-Ti oxides: Fe-Mg-Ti oxides and olivine. *Am Mineral 76:427-444*
- Anovitz LM (1991) Al-zoning in pyroxene and plagioclase: window on the late prograde to early retrograde  $P$ - $T$  paths in granulite terranes. *Am Mineral 76:1328-1343*
- Aranovich LY (1983) Biotite - garnet equilibria in metapelites. I. Thermodynamics of solid solutions and mineral reactions. In: Zharikov VV, Fed'kin V (eds) *Ocherki fiziko khimicheskoi petrologii*. Nauka Press, Moscow, pp 14-33
- Aranovich LY (1991) Mineral equilibria of multicomponent solid solutions. Nauka Press, Moscow
- Aranovich LY, Berman RG (1995)  $\text{Al}_2\text{O}_3$  solubility in orthopyroxene in equilibrium with almandine in the  $\text{FeO-Al}_2\text{O}_3\text{-SiO}_2$  system. *Current Res Geol Surv Can Pap 1995-E:271-278*
- Aranovich LY, Berman RG (1996) A new orthopyroxene-garnet thermometer, based on reversed  $\text{Al}_2\text{O}_3$  solubilities in orthopyroxene in the  $\text{FeO-Al}_2\text{O}_3\text{-SiO}_2$  system. *Am Mineral (in press)*
- Aranovich LY, Podlesskii KK (1989) Geothermobarometry of high-grade metapelites: simultaneously operating reactions. In: Cliff RA, Yardley BWD, Daly JS (eds) *Evolution of metamorphic belts*. Blackwell Scientific Publications, Oxford, pp 45-62
- Begin NJ, Pattison DRM (1994) Metamorphic evolution of granulites in the Minto block, northern Quebec: extraction of peak  $P$ - $T$  conditions taking account of late Fe-Mg exchange. *J Metamorphic Geol 12:411-428*
- Berg JH (1977) Regional geobarometry in the contact aureoles of the anorthositic Nain complex, Labrador. *J Petrol 18:399-430*
- Berman RG (1988) Internally-consistent thermodynamic data for minerals in the system  $\text{Na}_2\text{O-K}_2\text{O-CaO-MgO-FeO-Fe}_2\text{O}_3\text{-Al}_2\text{O}_3\text{-SiO}_2\text{-TiO}_2\text{-H}_2\text{O-CO}_2$ . *J Petrol 29:455-522*
- Berman RG (1991) Thermobarometry using multi-equilibrium calculations - a new technique, with petrological applications. *Can Mineral 29:833-855*

- Berman RG, Aranovich LY (1996) Optimized standard state and solution properties of minerals: I. Model calibration for olivine, orthopyroxene, cordierite, garnet, and ilmenite in the system  $\text{FeO}-\text{MgO}-\text{CaO}-\text{Al}_2\text{O}_3-\text{TiO}_2-\text{SiO}_2$ . *Contrib Mineral Petrol* 126: 1–24
- Bertrand P, Ellis DJ, Green DH (1991) The stability of sapphirine-quartz and hypersthene-sillimanite-quartz assemblages: an experimental investigation in the system  $\text{FeO}-\text{MgO}-\text{Al}_2\text{O}_3-\text{SiO}_2$  under  $\text{H}_2\text{O}$  and  $\text{CO}_2$  conditions. *Contrib Mineral Petrol* 108: 55–71
- Bishop FC (1980) The distribution of  $\text{Fe}^{2+}$  and Mg between coexisting ilmenite and pyroxene with application to geothermometry. *Am J Sci* 280: 46–77
- Bohlen SR, Boettcher AL (1981) Experimental investigations and geological applications of orthopyroxene geobarometry. *Am Mineral* 66: 951–964
- Bohlen SR, Essene EJ, Boettcher AL (1980) Reinvestigation and application of olivine-orthopyroxene-quartz barometry. *Earth Planet Sci Lett* 47: 1–10
- Bohlen SR, Wall VJ, Boettcher AL (1983) Experimental investigations and geological applications of equilibria in the system  $\text{FeO}-\text{TiO}_2-\text{Al}_2\text{O}_3-\text{SiO}_2-\text{H}_2\text{O}$ . *Am Mineral* 68: 1049–1058
- Chakraborty S, Ganguly J (1992) Cation diffusion in aluminosilicate garnets: experimental determination in spessartine-almandine diffusion couples, evaluation of effective binary diffusion coefficients, and applications. *Contrib Mineral Petrol* 111: 74–86
- Coolen JJM (1980) Chemical petrology of the Furua granulite complex, southern Tanzania. *GUA Pap Geol* 13: 1–258
- de Capitani C, Brown TH (1987) The computation of chemical equilibrium in complex systems containing non-ideal solutions. *Geochim Cosmochim Acta* 51: 2639–2652
- Eckert JO, Bohlen SR (1992) Reversed experimental determinations of the Mg- $\text{Fe}^{2+}$  exchange equilibrium in Fe-rich garnet-orthopyroxene pairs. *EOS Trans Am Geophys Union* 73: 608
- Ellis DJ, Sheraton JW, England RN, Dallwitz WB (1980) Osumilite-sapphirine-quartz granulites from Enderby Land, Antarctica-mineral assemblages and reactions. *Contrib Mineral Petrol* 72: 123–143
- Finnerty AA, Boyd FR (1984) Evaluation of thermobarometers for garnet peridotites. *Geochim Cosmochim Acta* 48: 15–27
- Fitzsimons ICW, Harley SL (1994) Disequilibrium during retrograde cation exchange and recovery of peak metamorphic temperatures: a study of granulites from Antarctica. *J Petrol* 35: 543–576
- Florence FP, Spear FS (1991) Effects of diffusional modification of garnet growth zoning on P-T path calculations. *Contrib Mineral Petrol* 107: 487–500
- Fonarev VI (1987) Mineral equilibria in Precambrian iron formations. Nauka Press, Moscow
- Fonarev VI, Korol'kov GJ, Dokina TN (1976) Stability of the orthopyroxene+magnetite+quartz association under hydrothermal conditions. *Geochem Int* 13: 134–146
- Frost BR, Chacko T (1989) The granulite uncertainty principle: limitations on thermobarometry in granulites. *J Geol* 97: 435–450
- Green DH, Sobolev NV (1975) Coexisting garnets and ilmenites synthesized at high pressures from pyrolite and olivine basanite and their significance for kimberlitic assemblages. *Contrib Mineral Petrol* 50: 217–229
- Harley SL (1984) The solubility of alumina in orthopyroxene coexisting with garnet in  $\text{FeO}-\text{MgO}-\text{Al}_2\text{O}_3-\text{SiO}_2$  and  $\text{CaO}-\text{FeO}-\text{MgO}-\text{Al}_2\text{O}_3-\text{SiO}_2$ . *J Petrol* 25: 665–696
- Harley SL (1989) The origins of granulites: a metamorphic perspective. *Geol Mag* 126: 215–247
- Harlov DE (1992) Comparative oxygen barometry in granulites, Bamble Sector, SE Norway. *J Geol* 100: 447–464
- Hayob JL, Bohlen SR, Essene EJ (1993) Experimental investigation and application of the equilibrium rutile+orthopyroxene=quartz+ilmenite. *Contrib Mineral Petrol* 115: 18–35
- Helgeson HC, Delany JM, Nesbitt HW, Bird DK (1978) Summary and critique of the thermodynamic properties of rock-forming minerals. *Am J Sci* 278A
- Hensen BJ (1976) The ability of pyrope-grossular garnet with excess silica. *Contrib Mineral Petrol* 55: 279–292
- Hensen BJ, Harley SL (1990) Graphical analysis of P-T-X relations in granulite facies metapelites. In: Ashworth JR, Brown M (eds) High-temperature metamorphism and crustal anatexis. Unwin Hyman, United Kingdom, pp 19–56
- Holland TJB, Powell RP (1990) An internally consistent thermodynamic dataset with uncertainties and correlations: the system  $\text{K}_2\text{O}-\text{Na}_2\text{O}-\text{CaO}-\text{MgO}-\text{MnO}-\text{FeO}-\text{Fe}_2\text{O}_3-\text{Al}_2\text{O}_3-\text{TiO}_2-\text{SiO}_2-\text{C}-\text{H}_2-\text{O}_2$ . *J Metamorphic Geol* 8: 89–124
- Jaffe HW, Robinson P, Tracy RJ (1978) Orthoferrosilite and other iron-rich pyroxenes in microperthite gneiss of the Mount Marcy area, Adirondack Mountains. *Am Mineral* 63: 1116–1136
- Jen LS, Kretz R (1981) Mineral chemistry of some mafic granulites from the Adirondack region. *Can Mineral* 19: 479–491
- Johnson CA, Essene EJ (1982) The formation of garnet in olivine-bearing metagabbros from the Adirondacks. *Contrib Mineral Petrol* 81: 240–251
- Karpov IK, Kiselev AI, Letnikov FA (1976) Computer modeling of natural mineral formation processes (in Russian). Nauka Press, Moscow
- Karsakov LP (1978) Deep-seated granulites (in Russian). Nauka Press, Moscow
- Kawasaki T, Matsui Y (1983) Thermodynamic analyses of equilibria involving olivine, orthopyroxene and garnet. *Geochim Cosmochim Acta* 47: 1661–1679
- Koch-Muller M, Cemic L, Langer K (1992) Experimental and thermodynamic study of Fe-Mg exchange between olivine and orthopyroxene in the system  $\text{MgO}-\text{FeO}-\text{SiO}_2$ . *Eur J Mineral* 4: 115–135
- Korzinskii DS (1973) Theoretical basis for analysis of parageneses of minerals (in Russian). Nauka Press, Moscow
- Koziol AM, Bohlen SR (1992) Solution properties of almandine-pyrope garnet as determined by phase equilibrium experiments. *Am Mineral* 77: 765–773
- Lamb RC, Smalley PC, Field D (1985) P-T conditions for the Arendal granulites, southern Norway: implications for the roles of P, T and  $\text{CO}_2$  in deep crustal LILE-depletion. *J Metamorphic Geol* 4: 143–160
- Lee HY, Ganguly J (1988) Equilibrium compositions of coexisting garnet and orthopyroxene: experimental determinations in the system  $\text{FeO}-\text{MgO}-\text{Al}_2\text{O}_3-\text{SiO}_2$ , and applications. *J Petrol* 29: 93–113
- Lindsley DH (1980) Phase equilibria of pyroxenes at pressures > 1 atmosphere. In: Prewitt CT (ed) Pyroxenes (Reviews in Mineralogy vol 7). Mineralogical Society of America, Washington DC, pp 289–308
- Matsui Y, Nishizawa O (1974) Iron(II)-magnesium exchange equilibrium between olivine and calcium-free pyroxene over a temperature range 800°C to 1300°C. *Bull Soc Fr Mineral Cristallogr* 97: 122–130
- Medaris Jr LG (1969) Partitioning of Fe and Mg between coexisting synthetic olivine and orthopyroxene. *Am J Sci* 267: 945–968
- Mora CI, Valley JW (1985) Ternary feldspar thermometry in granulites from the Oaxacan Complex, Mexico. *Contrib Mineral Petrol* 89: 215–225
- Newton RC (1972) An experimental determination of the high-pressure stability limits of magnesian cordierite under wet and dry conditions. *J Geophys Res* 80: 398–420
- Pattison DRM, Begin NJ (1994) Compositional maps of metamorphic orthopyroxene and garnet: evidence for a hierarchy of closure temperatures and implications for geothermometry of granulites. *J Geol* 12: 387–410
- Pattison DRM, Newton RC (1989) Reversed experimental calibration of the garnet-clinopyroxene Fe-Mg exchange thermometer. *Contrib Mineral Petrol* 101: 87–103
- Perchuk LL, Aranovich LY, Podlesskii KK, Lavrent'eva IV, Gerasimov VY, Kitsul VI, Korsakov LP, Berdnikov NV (1985) Precambrian granulites of the Aldan shield, eastern Siberia, the USSR. *J Metamorphic Geol* 3: 265–310

- Percival JA (1991) Granulite-facies metamorphism and crustal magmatism in the Ashuanipi Complex, Quebec Labrador, Canada. *J Petrol* 32: 1261–1297
- Perkins D (1983) The stability of Mg-rich garnet in the system CaO–MgO–Al<sub>2</sub>O<sub>3</sub>–SiO<sub>2</sub> at 1000–1300°C and high pressure. *Am Mineral* 68: 355–364
- Perkins DI, Essene EJ, Marcotty LA (1982) Thermometry and barometry of some amphibolite-granulite facies rocks from the Otter Lake area, southern Quebec. *Can J Earth Sci* 19: 1759–1774
- Powell R, Holland TJB (1985) An internally consistent thermodynamic dataset with uncertainties and correlations: 1. Methods and a worked example. *J Metamorphic Geol* 3: 327–342
- Powell R, Holland TJB (1988) An internally consistent thermodynamic dataset with uncertainties and correlations: 3. Applications to geobarometry, worked examples and a computer program. *J Metamorphic Geol* 6: 173–204
- Prigogine I, Defay R (1954) *Chemical thermodynamics*. Longmans, Norwich
- Sack RO, Ghiorso MS (1989) Importance of considerations of mixing properties in establishing an internally consistent thermodynamic database: thermochemistry of minerals in the system Mg<sub>2</sub>SiO<sub>4</sub>–Fe<sub>2</sub>SiO<sub>4</sub>–SiO<sub>2</sub>. *Contrib Mineral Petrol* 102: 41–68
- Sandiford M (1985) The metamorphic evolution of granulites at Fyfe Hills: implications for Archaean crustal thickness in Enderby Land, Antarctica. *J Metamorphic Geol* 3: 155–178
- von Seckendorff V, O'Neill HSC (1993) An experimental study of Fe–Mg partitioning between olivine and orthopyroxene at 1173, 1273 and 1473 K and 1.6 Gpa. *Contrib Mineral Petrol* 113: 196–207
- Wood BJ, Holloway JR (1984) A thermodynamic model for subsolidus equilibria in the system CaO–MgO–Al<sub>2</sub>O<sub>3</sub>–SiO<sub>2</sub>. *Geochim Cosmochim Acta* 48: 159–176